Potential of an emissive cylindrical probe in plasma

A. Fruchtman, D. Zoler,[*] and G. Makrinich

Faculty of Sciences, H.I.T. – Holon Institute of Technology, Holon 58102, Israel
(Received 23 January 2011; revised manuscript received 21 April 2011; published 8 August 2011)

The floating potential of an emissive cylindrical probe in a plasma is calculated for an arbitrary ratio of Debye length to probe radius and for an arbitrary ion composition. In their motion to the probe the ions are assumed to be collisionless. For a small Debye length, a two-scale analysis for the quasineutral plasma and for the sheath provides analytical expressions for the emitted and collected currents and for the potential as functions of a generalized mass ratio. For a Debye length that is not small, it is demonstrated that, as the Debye length becomes larger, the probe potential approaches the plasma potential and that the ion density near the probe is not smaller but rather is larger than it is in the plasma bulk.

The reduction of the potential drop between a material surface and a plasma when the material emits electrons has a dramatic effect on the wall-plasma interaction in fusion reactors [1], plasma processing [2], and electric propulsion [3]. In calculating the reduction of the potential drop for a certain configuration, the specific geometry and the presence of drifting plasmas have to be taken into account. We calculate here the reduction of the potential drop in a cylindrical emissive probe, an electron-emitting electrode that is a major tool for measuring plasma potential [4]. In a classic paper [5] Hobbs and Wesson calculated the potential drop across the (assumed narrow) sheath near an electron-emitting electrode and expressed the currents in terms of the plasma parameters at the sheath edge. However, the plasma potential can be evaluated only if the full potential drop between the emissive probe and the unperturbed plasma bulk is determined. Moreover, often the sheath near the probe is not narrow and the plasma is composed of more than one ion species [6]. In this Rapid Communication we calculate the potential drop between a cylindrical emissive probe and the unperturbed plasma bulk for an arbitrary ratio of Debye length to probe radius (the Debye number) and an arbitrary plasma ion composition. For a small Debye number we employ a two-scale analysis and derive analytical expressions for the potential drop and various currents. We then show numerically that when the Debye number is large, the probe potential approaches the plasma potential and the ion density near the probe is not smaller but rather is larger than it is in the plasma bulk.

Let us consider a cylindrical probe of radius a that is immersed in a plasma. We assume an azimuthal symmetry so that all variables depend on r only, the distance from the probe axis ($r \geqslant a$). Three particle groups contribute to the plasma charge and to the current to the probe. The first group is an arbitrary composition of ions of various (positive) charges and masses. The particle flux per probe unit length of the jth ion species is Γ_j and its density is $\overline{n}_j$. The second group is the plasma electrons whose flux per probe unit length is Γ_e and whose density is $\overline{n}_e$. The third group is the electrons emitted from the probe (with an assumed zero velocity) and accelerated

radially outward toward the higher-potential plasma. Their flux per probe unit length is Γ_c and their density is $\overline{n}_c$. The densities are

$$\overline{n}_j = \frac{\Gamma_j}{2\pi r(-2Z_j e\phi/M_j)^{1/2}},$$
$$\overline{n}_e = \frac{\Gamma_e}{2\pi a(v_t/4)} \exp\left(\frac{e(\phi - \phi_c)}{T}\right), \qquad (1)$$
$$\overline{n}_c = \frac{\Gamma_c}{2\pi r[2e(\phi - \phi_c)/m]^{1/2}},$$

where ϕ is the electric potential ($\phi = 0$ at the plasma bulk, where r is infinite), e is the elementary charge, $Z_j e$ is the charge, and M_j is the mass of the jth ion species. We assume that the ions move only radially inward in the direction of the probe axis without collisions, starting from rest at the plasma bulk. This is a good approximation in the common case that the ion-neutral collision mean free path is much larger than the width of the region around the probe, across which the potential drops, even if this mean free path is much smaller than the system size. The assumption of a pure radial motion corresponds to the so-called Allen-Boyd-Reynolds (ABR) theory [7] and was also used in Ref. [8] for a nonemissive cylindrical probe. The analysis can be extended to the orbital-motion-dominated regime [9]. Also $v_t = (8T/\pi m)^{1/2}$, with T being the electron temperature and m its mass, and ϕ_c denotes the (negative) potential at the probe.

Poisson's equation, divided by en_0 [with n_0 the plasma bulk density ($r \to \infty$)], becomes

$$\frac{\delta^2}{\xi}\frac{\partial}{\partial\xi}\left(\xi\frac{\partial\psi}{\partial\xi}\right) = n_t(\psi,\xi) \equiv \exp(\psi)$$
$$+ \frac{I_c}{\sqrt{4\pi}\xi(\psi - \psi_c)^{1/2}} - \frac{I_M}{\sqrt{4\pi}\xi(-\psi)^{1/2}}, \qquad (2)$$

while the equation for the current balance from the probe, divided by $e\Gamma_0$ [with $\Gamma_0 \equiv n_0(v_t/4)2\pi a$], becomes

$$I_T = \exp(\psi_c) - I_c - \frac{I_M}{\sqrt{\mu}}. \qquad (3)$$

The normalized potential and coordinate are $\psi \equiv e\phi/T$ (so that $\psi_c \equiv e\phi_c/T$) and $\xi \equiv r/a$, respectively. The terms on the right-hand side (rhs) of Eq. (2) are the dimensionless

---

[*]On leave from Propulsion Physics Laboratory, Soreq Nuclear Research Center, Yavne 81800, Israel.

charge densities $n_e \equiv \bar{n}_e/n_0$, $n_c \equiv \bar{n}_c/n_0$, and $n_i \equiv \Sigma \bar{n}_j/n_0$, respectively, and the terms on the rhs of Eq. (3) are the dimensionless currents $I_e \equiv \Gamma_e/\Gamma_0 = \exp(\psi_c)$ and $I_c \equiv \Gamma_c/\Gamma_0$ and the normalized ion current $I_i \equiv \Sigma Z_j \Gamma_j/\Gamma_0$ ($I_M \equiv I_i \sqrt{\mu}$), while I_T is the normalized total current. The two governing parameters in Eqs. (2) and (3) are δ, the Debye number, and μ, the generalized mass ratio, where

$$\delta \equiv \frac{\lambda_D}{a}, \quad \frac{1}{\sqrt{\mu}} \equiv \Sigma \frac{Z_j f_j}{\sqrt{\mu_j}}. \tag{4}$$

Here $\lambda_D \equiv \sqrt{T\epsilon_0/e^2 n_0}$ is the Debye length (ϵ_0 is the permittivity of free space), $\mu_j \equiv M_j/m$, and $f_j \equiv n_{j0}/n_0$ (n_{j0} is $\bar{n}_j$ at the plasma bulk). The effect of the ion mass, even of a multi-ion plasma, enters through a single parameter μ. The boundary conditions are $\psi(\xi = 1) = \psi_c$ and ψ and $\partial\psi/\partial\xi \longrightarrow 0$ as $\xi \longrightarrow \infty$. Once δ, μ, I_T, and I_c are specified, Eqs. (2) and (3) are solved for $\psi(\xi)$ and for ψ_c as an eigenvalue. We focus here on a floating probe $I_T = 0$. Solutions exist for I_c up to the space-charge limit (SCL), which is reached when $d\psi/d\xi = 0$ at the probe. Once I_M is specified, each ion-species flux is expressed as $\Gamma_j = I_M \Gamma_0 f_j/\sqrt{\mu_j}$.

We start by performing a two-scale analysis for the two plasma regions: the quasineutral plasma (presheath) and the non-neutral sheath adjacent to the probe, a generalization of the two-scale analysis made for the case of no electron emission [10]. The quasineutral plasma is described by the plasma equation $n_t = 0$ that is, [Eq. (2) in which we neglect the left-hand side]. In this equation ψ and ξ are related algebraically, $\xi = \xi(\psi)$. The plasma equation exhibits a singularity if the electric field becomes infinite ($d\xi/d\psi = 0$), resulting in

$$0 = \frac{I_c}{(\psi_s - \psi_c)^{1/2}} \left(1 + \frac{1}{2(\psi_s - \psi_c)}\right) - \frac{I_M}{(-\psi_s)^{1/2}} \left(1 + \frac{1}{2\psi_s}\right), \tag{5}$$

where ψ_s is the potential at this plasma-sheath boundary. We also write explicitly the plasma equation at that boundary $\xi = \xi_s$ as

$$0 = \exp(\psi_s) + \frac{I_c}{\sqrt{4\pi}\xi_s(\psi_s - \psi_c)^{1/2}} - \frac{I_M}{\sqrt{4\pi}\xi_s(-\psi_s)^{1/2}}. \tag{6}$$

When the Debye number is small $\delta \ll 1$, the non-neutral sheath is narrow and we approximate $\xi_s = 1$ in Eq. (6). We define a new coordinate $\zeta \equiv (\xi - 1)/\delta = (r - a)/\lambda_D$ and obtain the sheath equation [Eq. (2) in which we approximate $\xi = 1 + \delta\zeta \cong 1$]. We integrate the sheath equation from $\psi = \psi_s$, where we approximate $\partial\psi/\partial\zeta = 0$, so that $(1/2)(\partial\psi/\partial\zeta)^2 = g(\psi) \equiv \int_{\psi_s}^{\psi} n_t(\psi', \xi = 1)d\psi'$, and obtain at the probe

$$\frac{1}{2}\left(\frac{\partial\psi}{\partial\zeta}\right)^2_{\psi=\psi_c} = \exp(\psi_c) - \exp(\psi_s) - \frac{2I_c}{\sqrt{4\pi}}(\psi_s - \psi_c)^{1/2}$$
$$+ \frac{2I_M}{\sqrt{4\pi}}[(-\psi_c)^{1/2} - (-\psi_s)^{1/2}]. \tag{7}$$
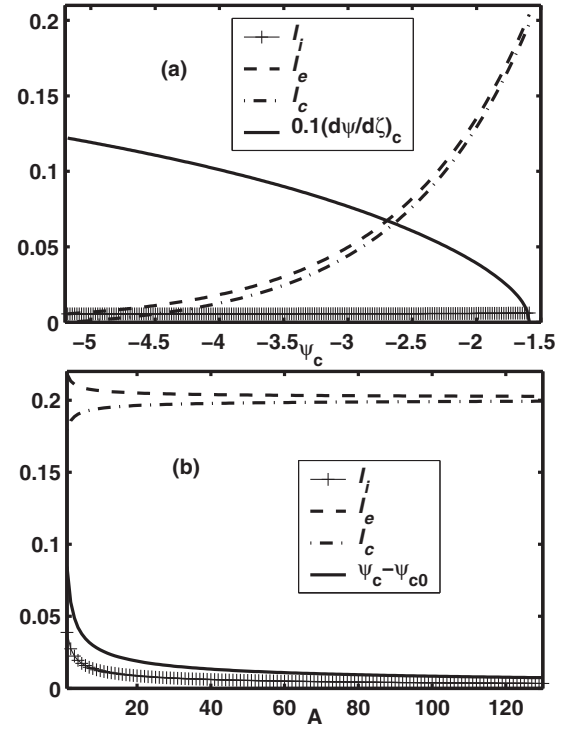

FIG. 1. Two-scale analysis for $\delta \ll 1$ ($I_T = 0$). (a) Dimensionless currents and electric field at the probe as functions of the probe potential ($\sqrt{\mu} = 271$ argonlike). When $I_c = 0$, I_i ($= I_M/\sqrt{\mu}$) $= I_e$, while at the SCL, $(d\psi/d\zeta)_c = 0$, $I_e \cong I_c \gg I_i$. (b) Dimensionless currents and probe potential at the SCL as functions of the effective atomic number $A \geqslant 1$ [$\psi_{c0} = \psi(A = \infty) = -1.6034$].

Equations (3), (5), (6) (with $\xi_s = 1$), and (7) are the governing equations of the two-scale analysis for $\delta \ll 1$. Figure 1(a) shows solutions of these equations for $I_c \geqslant 0$ for an argonlike plasma. The results hold for all ion compositions of the same μ, for example, a plasma of 82.8% Xe$^+$ and 11.2% He$^+$. When $I_c = 0$, we recover analytically the well-known relations for a nonemissive probe, extended to an arbitrary ion composition: $\psi_c = -0.5[1 + \ln(\mu/2\pi)]$, $\psi_s = -0.5$, and $I_e = I_i = 1.5203/\sqrt{\mu}$ (so that $\Gamma_j/\Gamma_0 = 1.5203 f_j/\sqrt{\mu_j}$). As I_c increases, I_e also increases and they both reach their maximal and close values when $(d\psi/d\varsigma)_{\psi=\psi_c} = 0$, at the SCL, while I_i ($= I_M/\sqrt{\mu}$) remains very small. At the plasma-sheath boundary, ψ_s (not shown) changes monotonically from $\psi_s = -0.5$ at $I_c = 0$ to $\psi_s = -0.5775$ at the SCL. The modification of ψ_s by the electron emission results in a modified Bohm velocity, which for the jth ion is $v_{Bj} = (-2Z_j T\psi_s/M_j)^{1/2}$, which is larger than $(Z_j T/M_j)^{1/2}$, the Bohm velocity with no emission. The momentum carried by the ions with the modified velocity is larger than that of the plasma electrons, which accounts also for the momentum of the emitted electrons.

Employing the two-scale analysis for $\delta \ll 1$, we now derive analytical approximate expressions for the potentials and the currents at the SCL (with $I_T = 0$). We expand the equations with respect to the small parameter $1/\sqrt{\mu}$. We first solve numerically the algebraic nonlinear zeroth-order equations, in which $1/\sqrt{\mu} = 0$. In that zeroth order, the ion current (not density) is zero and the electron currents balance each other. We then solve the linearized equations with respect to $1/\sqrt{\mu}$.

We therefore obtain general relations for an emissive probe at the SCL, expressed with the plasma-bulk parameters:

$$\psi_c = -1.6034 + \frac{3.6193}{\sqrt{\mu}}, \quad \psi_s = -0.5781 + \frac{0.1556}{\sqrt{\mu}},$$

$$I_c = 0.2012 - \frac{0.9348}{\sqrt{\mu}}, \quad I_e = 0.2012 + \frac{0.7282}{\sqrt{\mu}}, \quad (8)$$

$$I_i = \frac{1.6630}{\sqrt{\mu}}.$$

In addition, $\Gamma_j / \Gamma_0 = 1.6630 f_j / \sqrt{\mu_j}$. Figure 1(b) shows the dependence on the effective atomic number $A \equiv \mu m / M_p$ (M_p is the proton mass) according to Eq. (8). The variations are very small, except for I_i, which increases linearly with $1/\sqrt{A}$ from its zero value for infinite A. The variation of ψ_s is too small to be shown.

The sheath part of our solution coincides with that from Hobbs and Wesson [5]. For example, to first order in $1/\sqrt{\mu}$, Eq. (8) yields $I_c / I_e = 1 - 8.3 / \sqrt{\mu}$, as in Ref. [5]. The presheath size, however, is on the order of the probe radius even when the Debye number is very small. It is the converging cylindrical geometry, rather than collisions or ionization [11], that provides the drag necessary for the subsonic acceleration in the presheath, as it does in the converging part of Laval nozzle [12]. The governing equations in Ref. [5] include the Bohm condition [13], which is expected to be associated with the singularity in the plasma equation [11]. Indeed, the Bohm condition [13] is that in the series expansion of $g(\psi)$ at the plasma-sheath boundary, the coefficient in front of the second term, $\partial^2 g / \partial \psi^2 = \partial n_t / \partial \psi$ at $\psi = \psi_s$, be larger than or equal to zero. The plasma equation $n_t [\psi(\xi), \xi] = 0$ results in

$$\frac{d\xi}{d\psi} = -\frac{\partial n_t / \partial \psi}{\partial n_t / \partial \xi}. \quad (9)$$

This relation demonstrates that satisfying the Bohm condition with the equality sign (used in Ref. [5]) is equivalent to having a singularity in the plasma equation (which we used).

The variations of ψ_c and of the currents with δ and the radial profiles are explored in Figs. 2–4 through a full numerical solution of Eqs. (2) and (3). Specifying δ and looking for the SCL solutions, we solve the equations for two eigenvalues ψ_c and I_M. Figure 2(a) shows the potential profiles for three small values of δ. In the calculation of the profiles $\xi(\psi)$ by the plasma equation, we used I_M, I_c, and ψ_c found in the full numerical solution. As δ increases the sheath width [and ξ_s in Eq. (6)] increases and the values of ψ_c (hard to see in the figure) and of the currents (not shown) depart from the values provided by the two-scale analysis Eq. (8).

Figure 2(b) reveals additional features of the sheath not provided by the two-scale analysis. At the SCL the sheath is a (highly nonsymmetric) double layer. The negatively charged layer, bounded by the probe and the plane of charge neutrality $n_t = 0$ (where the electric field is maximal), is narrow with a width $\cong \delta$. The positively charged layer, which extends from that plane up to the quasineutral plasma, is much wider.

The case that the Debye number is not small is explored numerically in Figs. 3 and 4. Figure 3 shows the profiles for $\delta = 1$. The singularity in the plasma equation disappears and the plasma solution is regular up to the probe without the electric field becoming infinite. Note also that the ion
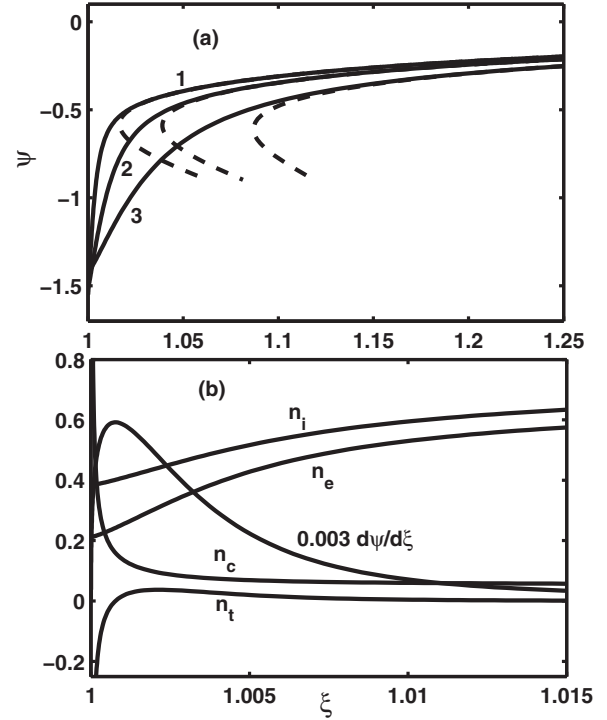

FIG. 2. Profiles at the SCL ($I_T = 0, \sqrt{\mu} = 271$) of (a) the potential for (1) $\delta = 0.001$ ($\psi_c = -1.551$), (2) $\delta = 0.003\,16$ ($\psi_c = -1.509$), and (3) $\delta = 0.01$ ($\psi_c = -1.42$) (dashed lines denote the corresponding solutions of the plasma equation) and (b) the particle densities and electric field for $\delta = 0.001$.
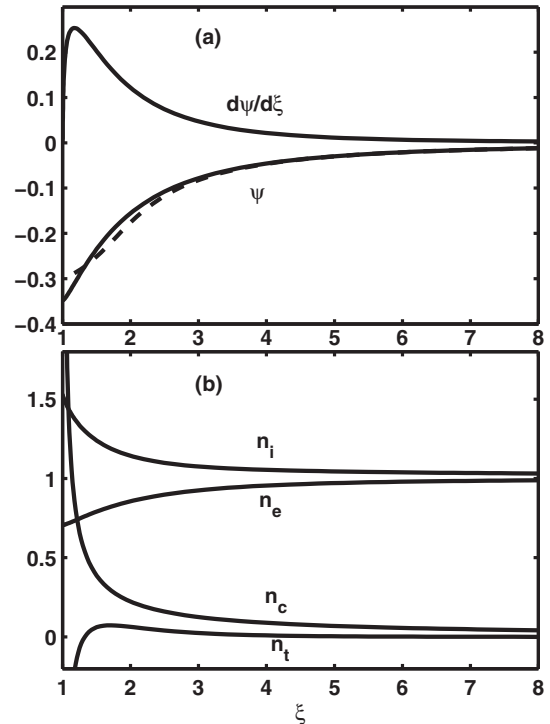

FIG. 3. Profiles at the SCL ($I_T = 0, \sqrt{\mu} = 271$) for $\delta = 1$ ($\psi_c = -0.348$) of (a) the potential and the electric field and (b) particle densities. The dashed line denotes the solution of the plasma equation, which is nonsingular for this case.
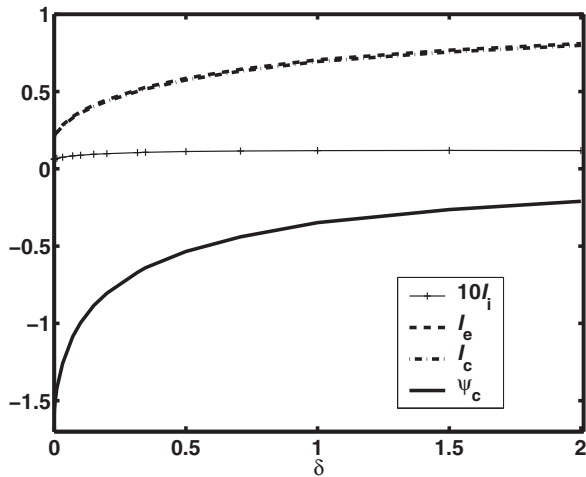
FIG. 4. Dimensionless currents and probe potential as functions of δ at the SCL ($I_T = 0$, $\sqrt{\mu} = 271$). The two electron currents are hardly distinguishable.

density does not decrease but rather increases as the probe is approached, being larger near the probe than it is in the plasma bulk. This ion density increase due to the geometric contraction for a large δ occurs also when the probe is not emitting (not shown here). The probe potential in the figure is much closer to the plasma potential than it is for a small δ.

Figure 4 shows how the probe potential decreases and the various currents increase with an increase of δ. The numerical calculation is quite general because it largely depends on one parameter only, on δ (the dependence on μ is weak). When δ is larger, the collected ion current and the emitted electron

current become larger. This forces the probe potential to get closer to the plasma potential so as to allow a larger electron current from the plasma to maintain a zero net current.

The fast decrease of ψ_c with δ reflects the dependence of ψ_c on the sheath size. For the sheath near a nonemitting surface, all matched asymptotic analyses [10,11,14], in spite of a certain controversy, suggest the presence of a transition layer that is described by a solution of the Painlavé equation of the first kind and that its size is proportional to δ^p ($p < 1$). The structure of the positive layer in the sheath in the SCL case is expected to be similar. Indeed, the sheath size $\xi_s - 1$ in Fig. 2(a) is much larger than δ. It follows from Eqs. (5) and (6) that $\psi_c - \psi_c(\delta = 0)$ is linearly proportional to $\xi_s - 1$. Therefore, $\psi_c - \psi_c(\delta = 0)$ is also expected to be proportional to δ^p ($p < 1$). Such a dependence results in an infinite derivative of ψ_c with respect to δ at $\delta = 0$, as indicated by the numerical solution in Fig. 4.

In summary, we calculated the potential of a cylindrical emissive probe for arbitrary Debye number and ion composition. For a small Debye number we derived analytical results. The collapse of the potential drop for a large Debye number suggests that it is beneficial to use a thinner emissive probe for a more accurate measurement of the plasma potential. The analysis could be extended to address the effects of a virtual cathode [15], finite probe length, and plasma drift, as well as the stability issue [6,16].

[1] N. Schupfer *et al.*, Plasma Phys. Control. Fusion **48**, 1093 (2006).

[2] X.-C. Li and Y.-N. Wang, Thin Solid Films **506-507**, 307 (2006).

[3] Y. Raitses, D. Staack, A. Smirnov, and N. J. Fisch, Phys. Plasmas **12**, 073507 (2005).

[4] N. Hershkowitz, in *Plasma Diagnostics, Discharge Parameters and Chemistry*, edited by O. Auciello and D. L. Flamm, Vol. 1, Chap. 3 (Academic, Boston, 1989).

[5] G. D. Hobbs and J. A. Wesson, Plasma Phys. **9**, 85 (1967).

[6] C.-S. Yip, N. Hershkowitz, and G. Severn, Phys. Rev. Lett. **104**, 225003 (2010).

[7] J. E. Allen, R. L. F. Boyd, and P. Reynolds, Proc. Phys. Soc. London Sect. B **70**, 297 (1957).

[8] F. F. Chen and D. Arnush, Phys. Plasmas **8**, 5051 (2001).

[9] I. B. Bernstein and I. N. Rabinowitz, Phys. Fluids **2**, 112 (1959); J. G. Laframboise and L. W. Parker, *ibid.* **16**, 629 (1973);

J. E. Allen, Physica Scripta **45**, 497 (1992); Z. Sternovsky and S. Robertson, Phys. Plasmas **11**, 3610 (2004).

[10] R. N. Franklin and J. R. Ockendon, J. Plasma Phys. **4**, 371 (1970).

[11] K.-U. Riemann, J. Phys. D **24**, 492 (1991).

[12] A. Fruchtman, N. J. Fisch, and Y. Raitses, Phys. Plasmas **8**, 1048 (2001).

[13] D. Bohm, in *Characteristics of Electrical Discharges in Magnetic Fields*, edited by A. Guthrie and R. K. Wakerling (McGraw-Hill, New York, 1949).

[14] V. A. Godyak and N. Sternberg, IEEE Trans. Plasma Sci. **18**, 159 (1990); R. N. Franklin, J. Phys. D **36**, R309 (2003).

[15] L. A. Schwager, Phys. Fluids B **5**, 631 (1993).

[16] S. D. Baalrud, C. C. Hegna, and J. D. Callen, Phys. Rev. Lett. **103**, 205002 (2009).